



Airborne pollutant dilution inside the deep street canyons subjecting to thermal buoyancy driven flows: Effects of representative urban skylines



Shuo-Jun Mei^{a,b,c}, Jiang-Tao Hu^{a,b,c}, Di Liu^{d,**}, Fu-Yun Zhao^{a,b,c,*}, Yuguo Li^e, Han-Qing Wang^f

^a Key Laboratory of Hydraulic Machinery Transients (Wuhan University), Ministry of Education, Wuhan, Hubei Province, China

^b Shenzhen Research Institute, Wuhan University, Shenzhen, Guangdong Province, China

^c School of Power and Mechanical Engineering, Wuhan University, Wuhan, Hubei Province, China

^d College of Pipeline and Civil Engineering, China University of Petroleum, Qingdao, Shandong Province, China

^e Department of Mechanical Engineering, The University of Hong Kong, Pokfulam Road, Hong Kong, China

^f School of Civil Engineering, University of South China, Hengyang, Hunan Province, China

ARTICLE INFO

Keywords:

Thermally-driven canyon ventilation
Urban morphology
Pollutant retention time
Thermal boundary layer flows
Thermal plume merging

ABSTRACT

The air flow and pollutant dispersion within a group of street canyons ventilated merely by thermal buoyancy force induced by heated building surfaces are examined by CFD model using SST $k-\omega$ turbulence model for different urban skyline configurations. Pollutants emitted from the bottom of street canyon roughly mimic the traffic exhaust releasing. Numerical results are validated well with former theoretical results on thermal boundary flow adjacent to a heated vertical wall. The air exchange rate per hour (ACH) and pollutant retention time are adopted to evaluate the canyon ventilation performance. An exponential relationship could be established between the pollutant retention time and the thermal boundary flow rate. A semi-empirical formula is proposed by using the theoretical results of thermal boundary layer and two empirical constants derived from the present simulation results, which could be used to evaluate the ventilation performance at the urban design. As the convergence flow at the street canyon roof decays from urban rim to urban center, the pollutant retention time differs from canyon to canyon. The “protuberant” skyline configuration is found more effectively in purifying the street canyons at urban edge, in contrast, the “concave” skyline configuration shows higher purification efficiency at urban center. Present research could benefit for design purpose and environmental impact assessment.

1. Introduction

Cities are now home to half of the world's 6.6 billion humans. By 2030, nearly 5 billion people will live in cities. City offers the opportunity of high quality of life: access to goods; service and resources; security and social organization [1]. However, urban inhabitants are also suffering from a wide range of air pollution, which is associated with a broad spectrum of acute and chronic health effects [2]. In order to improve urban air quality, there is a clear need for basic scientific understanding of the mixing and transport of airborne pollutants within urban area.

The air flow at urban area is driven by a combination of background wind, surface heating, moving traffic, all within a complex network of streets and buildings [3]. The interaction between the urban surface and the background wind has a significant effect on urban pollutants dispersion and thermal environment. In the past two decades, there is a

growing body of literature addressed the impact of groups of buildings on the air exchange and pollutant dispersion within the urban canopy layer (UCL). For the complexity of urban geometries, it is still very difficult to fully disclose all details of a realistic city. Therefore, idealized geometries are then used for parametric investigations. The urban morphology is a combination of generic characteristics of these geometries, which includes the urban density [4], the arrangement of buildings [5] and their individual shape and dimensions [6], street and building aspect ratios [7], overall urban forms [8], urban size (i.e. total street length [9]), building height variations [10], building dimensions [11], and etc. The number and arrangement of vortex structures within the street canyon can be largely influenced by the urban morphology [12], consequently, the exchange processes within the urban canopy layer (UCL) and urban air quality [13].

The flow and pollutant dispersion are significantly influenced by different urban morphologies and ambient wind directions. Kim and

* Corresponding author. School of Power and Mechanical Engineering, Wuhan University, Dong-Hu South Road, 430072, Wuhan, Hubei Province, PR China.

** Corresponding author.

E-mail addresses: liudi66@163.com (D. Liu), fyzhao@whu.edu.cn (F.-Y. Zhao).

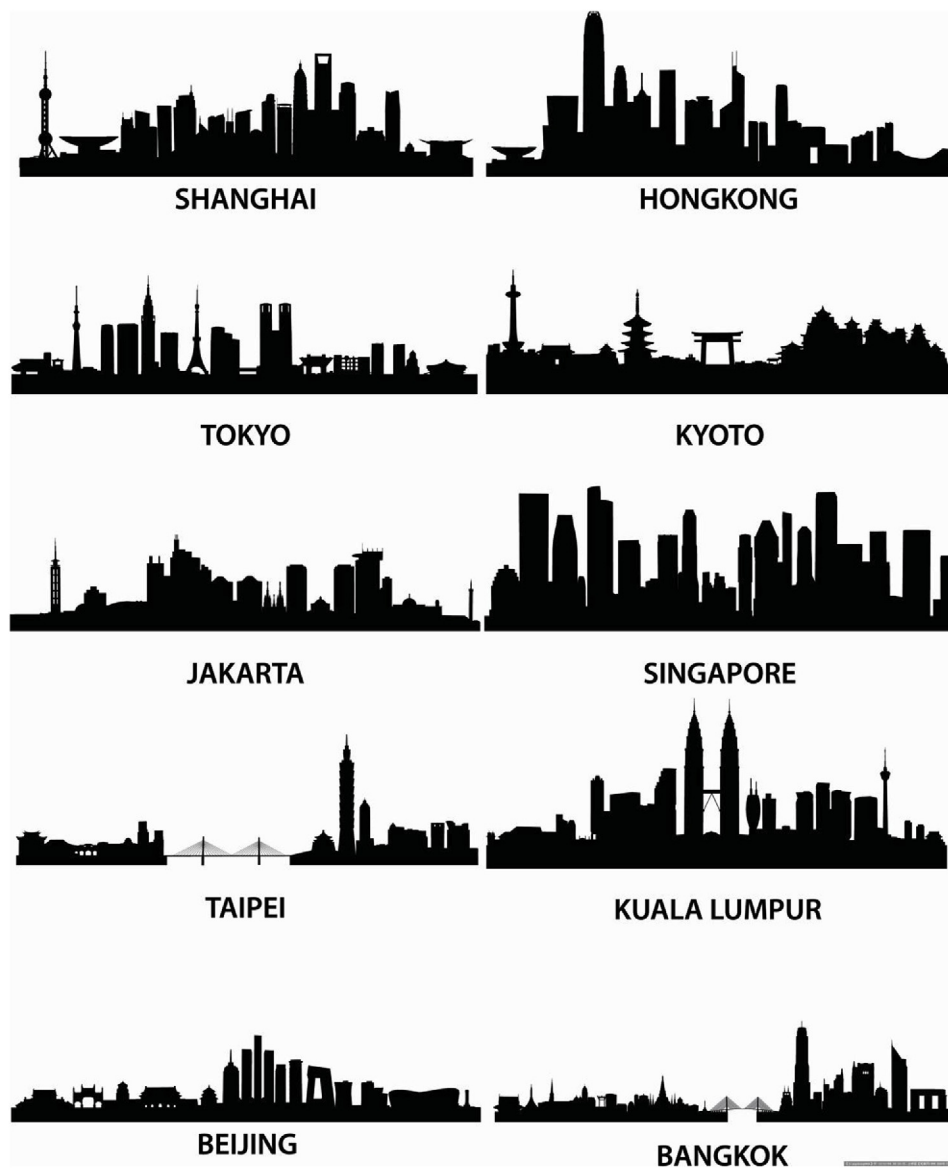


Fig. 1. General presentation of the skylines at ten different representative cities in the world.

Baik (2004) [14] reported that changes in ambient wind direction could result in huge differences in the mean turbulent flow circulation and the spatial distribution of passive pollutants. Di Sabatino et al. (2007) [15] found that the dispersion within real street canyons was influenced by the turbulence structure determined by the interaction between the flow and buildings. Hang et al. (2009) [16] found significant differences in air exchange efficiency between round and square cities. Buccolieri et al. (2010) [4] showed that the packaging density significantly changed the ventilation performance of an idealized building cluster. Branford et al. (2011) [17] have observed that topological dispersion raised when the building layout in a staggered arrangement with respect to the oncoming flow direction. Hang et al. (2012) [10] found that building arrays with varying height experienced better pedestrian ventilation than those with uniform height. Coceal et al. (2014) [18] summarized the processes that the presence of buildings affects the pollutant dispersion in the near field. Firstly, diverging streamline around buildings lead to considerable mean transport and enhanced lateral dispersion, Secondly, trapping and re-releasing of pollutants in the wake of buildings in the immediate vicinity of the release gives rise to secondary source.

The background wind considered in these investigations is

commonly assumed as moderate or strong. In addition to the background wind, heated building surface or street canyon bottom by solar radiation is found playing an important role in determining the flow patterns in UCL [19]. Materials with low heat capacity such as concrete and asphalt are widely used in modern urban construction. Thus, the building surfaces and street canyon bottom can be easily heated by intense solar radiation. Nakamura and Oke (1988) [20] showed that the maximum temperature difference between the building surface and air was achieved around 12–14° C. The numerical results of literature [21] exhibited that the differential heating of street surfaces could largely influence the flow's capability to transport and exchange pollutants. The further wind tunnel experiment [22] supported these results well. The numerical modeling [23] showed that a strong buoyant force was generated close to the ground by solar radiation. The primary vortex in the core of the street canyon could be divided into two vortices by the interaction between the buoyancy-induced flow and mechanical-induced flow. The observation from a field experiment [24] suggested that the urban air was mainly driven by the winds when ambient wind was higher than 4.0 m/s, whereas mainly being driven the thermal buoyancy when the natural wind flow speed was no more than 0.2 m/s. Barlag and Kuttler (1991) [25] suggested that thermal buoyancy

exerted a dominant influence on the urban air flow when the approaching wind speed was less than 2.5 m/s. Georgakis and Santamouris (2006) [26] carried out a measurement in a deep canyon in Athens during the summer period. They found that the air flow inside the canyon was not driven by the wind flow above the canyon when the wind speeds were lower than 5 m/s; instead, the thermal phenomena and intermittent vortices developed at the canyon corners dominate the air flow patterns inside the canyon.

Compared to wind speed, non-dimensional numbers can precisely evaluate the importance of buoyancy. In General, Richardson number ($Ri = g\beta H(T_0 - T_{ref})/(U_{ref}^2)$), where T_{ref} is the reference temperature and T_0 the temperature at the wall, U_{ref} the reference velocity, β the thermal expansion rate of air) or Froude number ($Fr = Ri^{-1}$) are used to quantify the relative importance of wind-driven force and buoyancy-driven force. Three situations can be classified, i.e. buoyancy-driven force dominates as $Ri < 0.5$ – 1.0 [27]; wind-driven force dominates as $Ri > 8$ [28]; both forces are significant as $0.5 < Ri < 8$. When buoyancy force dominant, upward flow could be observed near heated wall. The vertical velocity of this kind of flow was found about 1.0–2.0 m/s along a 60 m height building walls [29]. These upward flows could also interact with each other. Yin et al. (2017) [30] examined the merging process of triple building plumes using 2-D particle image velocimetry (PIV) measurements. Their results showed that multiple building plumes from the building cluster interacted with each other, forming neighbourhood scale merging problem.

Despite the increasing literature on urban dispersion, it is clear that important gaps remain in our fundamental understandings. In particular, pollutant dilution under weak background wind is a little-understood subject. However, heat and pollutant are much more likely to get accumulated at low wind speed scenario [31], creating the harshest urban air environment. As noted by previous studies [7,32], the high-rise buildings at urban edge prolong the retention time of pollutants inside the downstream street canyons. In the view of urban design application, more detailed studies of such cases are essentially required.

The urban skyline is a panoramic snapshot of the city's esthetic values, diversity, integrity, the history of its buildings and geographical elements [33]. General presentation of the skylines at ten different representative cities in the world has been presented in Fig. 1. The city skyline is an important node on which to focus for the development of proper control mechanisms, particularly concerning the vertical development of structures that can significantly impact the skyline. At wind driven urban ventilation, many neighbourhood-scale heterogeneities exert strong influence on urban canopy layer ventilation, for example, the building height variation [10,32,34], aspect ratio [24,35] and building size [7]. However, it is quite remarkable that none of them considered urban configurations consisting of different skyline forms. Therefore, multiple categories of urban skyline are considered in this study.

This paper aims to evaluate the dispersion of pollutants emitted at near ground level, which will be purely driven by thermal buoyancy forces induced by heated building exterior surfaces and street canyon bottom. A CFD model was then developed to investigate the wind and pollutant transport in the idealized street canyons with simulations at different representative urban skyline simultaneous heated on all the ground and façade surfaces.

2. Mathematical model

As background wind is assumed as zero, the air flow is only driven by buoyancy force. Previous studies suggested that the steady Reynolds-averaged Navier-Stokes (RANS) model was unable to capture the unsteadiness of the thermal turbulent plume [36]. Hence, an Unsteady Reynolds-averaged Navier-Stokes (URANS) model is applied.

2.1. Governing equations

As suggested by previous studies [19,28], the city could be assumed as aggregation of many infinitely long street canyons. The three-dimensional spatial domain could be simplified to a two-dimensional one. As the difference between the actual air density and the standard aerostatic density is small, the Boussinesq approximation is used here to calculate the buoyancy force. The atmospheric air can then be assumed incompressible. In 2-D RANS modeling, the flow properties are disintegrated into their mean and fluctuating components by Reynolds decomposition and substituted in the Navier–Stokes equations, which could be written as:

$$\frac{\partial \bar{u}_i}{\partial x_i} = 0 \quad (1)$$

$$\frac{\partial \bar{u}_i}{\partial t} + \frac{\partial}{\partial x_j}(\bar{u}_i \bar{u}_j) = -\frac{\partial \bar{p}_d}{\rho_n \partial x_i} + \frac{\partial}{\partial x_i}(\bar{T}_{ij} - \bar{u}'_i \bar{u}'_j) - g_i n_i \beta (\bar{T} - T_0) \quad (2)$$

$$\frac{\partial \bar{T}}{\partial t} + \frac{\partial}{\partial x_j}(\bar{u}_j \bar{T}) = \frac{\partial}{\partial x_j} \left(\frac{\mu}{Pr} \frac{\partial \bar{T}}{\partial x_j} - \bar{u}'_j \bar{T}' \right) \quad (3)$$

$$\frac{\partial \bar{C}}{\partial t} + \frac{\partial}{\partial x_j}(\bar{u}_j \bar{C}) = \frac{\partial}{\partial x_j}(-\bar{u}'_j \bar{C}') \quad (4)$$

where x_i are the Cartesian coordinates. The mean and fluctuating components of flow properties are marked with overbar and apostrophe respectively. For example, \bar{u}_i represents the components of the mean velocity, \bar{T} the mean air temperature and \bar{C} is the mean passive pollutant. Here, $g_i = (0, -g)$ is the gravitational acceleration, β the thermal expansion ratio, n_i the unit vector at vertical direction, Pr the Prandtl number, ρ_n the reference density of air, $\bar{u}'_i \bar{u}'_j$ the Reynolds stress tensor and $\bar{u}'_j \bar{T}'$ the turbulent heat flux. Here, $p_d = p - \rho_n g n_i$ is part of the piezometric pressure (p) which remains after the hydrostatic pressure is removed. The Reynolds stress tensor appearing in the mean momentum equation is modelled using the Boussinesq's eddy viscosity model:

$$-\bar{u}'_i \bar{u}'_j = 2\nu_t \bar{S}_{ij} - \frac{2}{3}k \delta_{ij} \quad (5)$$

where the strain rate tensor $\bar{S}_{ij} = \frac{1}{2} \left(\frac{\partial \bar{u}_i}{\partial x_j} + \frac{\partial \bar{u}_j}{\partial x_i} \right) - \frac{1}{3} \left(\frac{\partial \bar{u}_l}{\partial x_l} \right) \delta_{ij}$, k denotes the turbulent kinetic energy and ν_t the turbulent viscosity, which is calculated by the SST k - ω turbulent model. The turbulent heat flux is closed as:

$$-\bar{u}'_i \bar{T}' = -\frac{2}{3} \frac{\mu_t}{\sigma_t} \frac{\partial \bar{T}}{\partial x_j}, \quad (6)$$

and the turbulent pollutant flux is closed as:

$$-\bar{u}'_i \bar{C}' = -\frac{2}{3} \frac{\mu_t}{\sigma_t} \frac{\partial \bar{C}}{\partial x_j} \quad (7)$$

2.2. Turbulence model

SST (Shear Stress Transport) k - ω turbulence model has shown good performance in typical buoyant-driven flow [37]. It has been especially designed for predicting adverse pressure gradient flows where most of the two-equation models, and even higher-order models, are known to fail severely. The k - ω equations are applied only inside the boundary layers and the standard k - ϵ model is utilized elsewhere. This is because the pure k - ω model is known to be harmfully sensitive to the freestream turbulence, whereas the standard k - ϵ model does not share this defect with the k - ω model. The SST formulation switches to a k - ϵ behaviour in the free-stream, which avoids the deficient of standard k - ω model. Menter (1994) [38] developed a blending function that is equal to one in the inner region and goes gradually towards zero near the edge of the boundary layer.

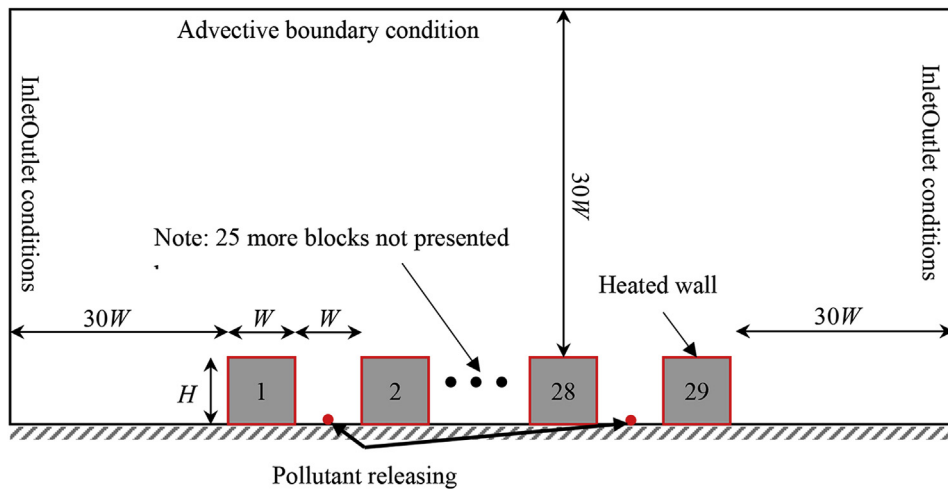


Fig. 2. Schematic diagram of configuration of the computational domain, canyon geometry and location of the point emission source on the street. The building surfaces are assumed to be heated by solar radiation. Building height and width are H and W , respectively.

2.3. Computational domain and boundary conditions

The computational domain is depicted in Fig. 2. The underlying geometry was the same in each simulation, consisting of rectangular obstacles with heated surfaces with the spacing between the obstacles ('streets') being equal to the width of building blocks (W) of 30 m. There are total 29 building blocks at each run, with a spanwise (x coordinate) range of 1.68 km, representing a typical urban neighbourhood. The urban blocks are assumed to be symmetric. Although the real urban area is asymmetric and irregular, a simplified symmetrical urban configuration still has the potential to reveal several basic flow and dispersion mechanisms at real scenarios. At the following sections, the "urban edge" refers to the areas close to the first or last building block and the "urban center" refers to the areas near the symmetric axis of the urban area. Different combinations of building heights constitute various urban skyline forms. There are three representative skyline forms considered in this study, which includes the "zigzag", the "protuberant", and the "concave", shown in Fig. 3. For the zigzag skyline form, the standard deviation σ_h of building heights is defined by Jiang et al.

(2008) [39] as

$$\sigma_h = \sqrt{\frac{1}{n} \sum_{i=1}^n \left(\frac{h_i - H}{H} \right)^2}, \quad (8)$$

where H is the average height of building arrays, h_i is the height of each building in the arrays. The runs are named in the form of $\sigma_h\text{-TE}$, where TE is the temperature elevation of the heated surfaces. The buildings are assumed located at a quiescent environment. The ambient air is maintained at a temperature of 300 K, and the building surfaces and streets are assumed be heated to a temperature ranging from 301 to 330 K. The vehicular pollutant is modelled by a hypothetical ground-level continuous pollutant point source placed at the street axis with an emission rate of Q_{emits} ($= 12 \mu\text{g m}^{-3} \text{s}^{-1}$), which is also used in the former work [40]. The pollutants are assumed to be dispersing passively. The distance between the side boundaries and the urban edge is 30W, which is to create a quiescent environment [41]. Neumann zero-normal-derivative conditions were applied to scalar transfer on the upper, lower, side and wall boundaries, and condition $C = 0$ was imposed on the side boundaries of the domain. The initial turbulent

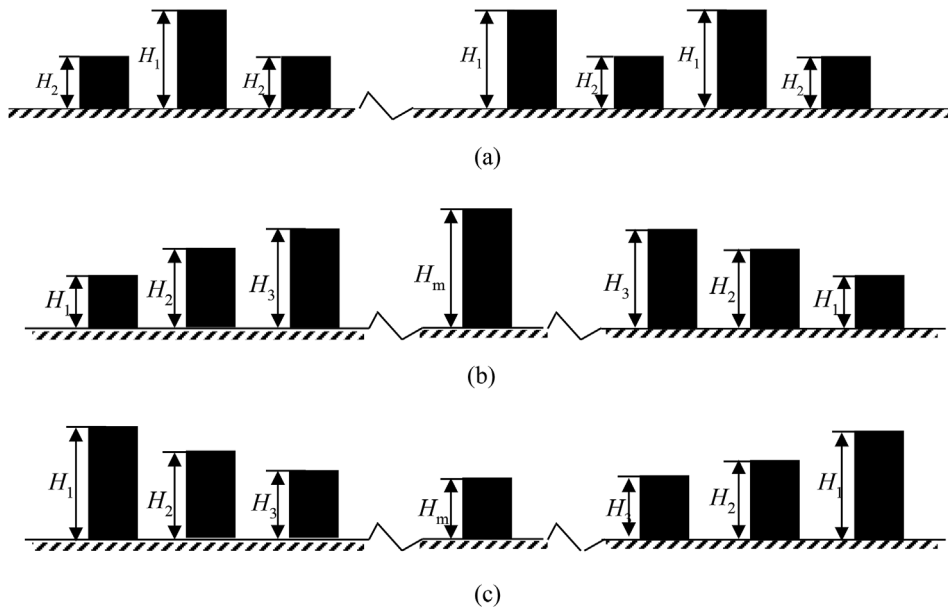


Fig. 3. Schematic diagram of the configurations of three basic skyline types considered in this study, which includes the "zigzag" (a), the "protuberant" (b), and the "concave" (c). At each configuration, 29 buildings are included.

Table 1

Summary of building configuration considered in this study. Building height, where W (= 30 m) is the street width.

Zigzag skyline													
H_1/W	1		0.9		0.8		0.7		0.6		0.5		0.4
H_2/W	1		1.1		1.2		1.3		1.4		1.5		1.6
σ_h	0		0.1		0.2		0.3		0.4		0.5		0.6
Protuberant skyline													
Block	1	2	3	4	5	6	7	8	9	10	11	12	13
H/W	1.0	1.1	1.2	1.3	1.4	1.5	1.6	1.7	1.8	1.9	2.0	2.1	2.2
Block	16	17	18	19	20	21	22	23	24	25	26	27	28
H/W	2.3	2.2	2.1	2.0	1.9	1.8	1.7	1.6	1.5	1.4	1.3	1.2	1.1
concave skyline													
Block	1	2	3	4	5	6	7	8	9	10	11	12	13
H/W	2.4	2.3	2.2	2.1	2.0	1.9	1.8	1.7	1.6	1.5	1.4	1.3	1.2
Block	16	17	18	19	20	21	22	23	24	25	26	27	28
H/W	1.1	1.2	1.3	1.4	1.5	1.6	1.7	1.8	1.9	2.0	2.1	2.2	2.3

Table 2

Summary of the boundary conditions.

	Side	Top	Bottom	Urban Surfaces
Velocity	Neumann	Advective	noSlip	noSlip
T	Neumann	Advective	Constant	Constant
Pressure (p)	Neumann	Neumann	Neumann	Neumann
Pressure(p_d)	Constant	Neumann	Condition 2	Condition 2
ε	Condition 1	Condition 1	Wall Function	Wall Function
k	Condition 1	Condition 1	Wall Function	Wall Function
ν_t	Neumann	Neumann	Wall Function	Wall Function

kinetic energy (k) and its dissipation rate (ε) were set as $10^{-6} \text{ m}^2/\text{s}^2$ and $10^{-9} \text{ m}^2/\text{s}^3$, respectively. More details about boundary conditions are given at Table 2. The details of the boundary conditions used in this paper are described at Table 3. These boundary conditions have also been adopted by previous simulations for pure buoyancy driven flow at quiescent environment [41]. (see Table 1)

2.4. Numerical methodology

The set of governing equations are discretized on a standard Cartesian two-dimensional grid, with pressure and temperature discretized on the cell center and velocity components discretized on the cell faces. The grid number within each street canyon is 100×100 . The near wall region was refined with an expand ratio of 1.1 to a level of $y^+ < 1$ for the first-layer cells to guarantee near wall processes are well captured. The pressure and temperature were discretized on the cell center and the velocity components were discretized on the cell faces. The unsteady equations were discretized using the implicit Euler's scheme. The second order upwind scheme was implemented for the gradients terms and the Gauss linear uncorrected scheme was used for the Laplacian terms. The momentum equations and pressure equations were decoupled using PISO algorithm. The convergence criterion for the residual of each equation was set as 10^{-6} . An adjustable time step was used with a maximum Courant number of 0.5. The total

computational time was $100 L/V_{\max}$, where L denotes the urban breadth and V_{\max} the maximum velocity, which is calculated by previous empirical formulas [42] on the turbulent free-convection boundary on a vertical plate. The computational components were averaged during the last $50 L/V_{\max}$ seconds.

2.5. Numerical test

Due to there is a lack of experiment on urban airflow driven by purely thermal buoyancy force, the numerical model is validated by comparing the results of near wall flow to the previous empirical formulas as a compromise. As the near wall flow is the basic element of the urban flow driven by thermal buoyancy force, this comparison could be used to prove the validity of the present CFD model.

In order to test the capability of turbulent models in calculating the near wall flow and heat transfer, a test case with a single building bounded at adiabatic floor was built. The computational domain and boundary conditions are identical to that in the building simulation cases described above.

Several parameters related to heat transfer are defined before introducing the empirical formulas. The Prandtl numbers is defined as $\text{Pr} = \nu/\alpha$, where ν and α are the kinematic viscosity the thermal diffusivity respectively. The Grashof number is defined as $\text{Gr} = gH^3\beta\Delta T/\nu^2$, where ΔT is the temperature differences between heated wall to the ambient air and β the expansion ratio of air. The Rayleigh number is defined as the $\text{Ra} = gH^3\beta\Delta T/(\alpha\nu)$.

Eckert and Jackson (1950) [42] derived the velocity and temperature profiles in the turbulent free-convection boundary on a vertical plate by using Kármán's integrated momentum equation. The velocity profile that represents the velocity for values of s less than δ (s is the coordinate distance from wall and δ is the boundary layer thickness) is

$$V = V_1 \left(1 - \frac{s}{\delta}\right)^4 \left(\frac{s}{\delta}\right)^{1/7}, \quad (9)$$

where

Table 3

Explanations of boundary conditions at OpenFOAM employed in the present work.

Boundary condition	Explanation
Condition 1	It provides a generic outflow condition, with specified inflow as constant value of zero for the case of return flow.
Condition 2	It assumes the pressure gradient to the provided value such that the flux on the boundary is that specified by the velocity boundary condition.
Wall Function for ε	It provides a turbulence dissipation wall constraint with the "Equilibrium assumption": $P_k = \nu_t \left(\frac{\partial U}{\partial y}\right)^2 = \varepsilon$, where P_t is the production term of turbulent kinetic energy due to shear.
Wall Function for k	It is a simple wrapper around the zero-gradient condition.
Advection	It provides an advective outflow condition, based on solving $\text{DDt}(W, \text{field}) = 0$ at the boundary where W is the wave velocity and field is the field to which this boundary condition is applied.

$$V_1 = 1.185 \frac{v}{H} (Gr)^{1/2} [1 + 0.494(\text{Pr})^{2/3}]^{-1/2}, \quad (10)$$

and

$$\delta = 0.565H(Gr)^{-1/10}(\text{Pr})^{-8/15}[1 + 0.494(\text{Pr})^{2/3}]^{1/10} \quad (11)$$

The volume flow rate of the wall flow Q , which is defined as $Q = \int_0^\infty V ds$, can be calculated as:

$$Q = 0.146V_1\delta \quad (12)$$

The maximum velocity V_{\max} of this profile can be found by differentiating Eq. (6) as $V_{\max} = 0.537V_1$. For fluids with a Prandtl number equal to 1, the temperature profile is similar in shape to the velocity profile and the expression is

$$T - T_\infty = (T_0 - T_\infty) \left[1 - \left(\frac{s}{\delta} \right)^{1/7} \right] \quad (13)$$

This correlation holds for $10^{-1} < Ra < 10^{12}$ and for all Prandtl numbers, where $Gr = Ra/\text{Pr}$.

The averaged Nusselt number ($Nu_{av} = q/\Delta T/k$, where q is the heat flux of the heated wall and k is the heat conductivity of air) represents the surface heat transfer rate of the heated wall. An empirical isothermal-wall correlation that reports the wall-averaged Nusselt number (Nu_{av}) for the entire Rayleigh number range – laminar, transition turbulent was constructed by Ref. [43].

$$Nu_{av} = \left\{ 0.825 + \frac{0.387Ra^{1/6}}{[1 + (0.492/\text{Pr})^{9/16}]^{8/27}} \right\}^2 \quad (14)$$

The Nu_{av} of a heated vertical wall with Grashof number ranging from 5×10^7 to 5×10^{14} is calculated with both SST $k-\omega$ and realizable $k-\epsilon$ model and compared to the empirical correlation. The Grashof number used in the present urban simulation ranges from 8×10^{12} to 1.5×10^{14} depending on the building height and wall temperature, which is within the tested Gr range. It is clear that the agreement between the SST $k-\omega$ and empirical correlation is good. However, the realizable $k-\epsilon$ model could only reproduce the Nusselt number of the heated wall when Grashof number is below 5×10^{11} .

The profiles of the non-dimensional vertical velocity and temperature obtained with $Gr = 5 \times 10^{11}$ are compared to the empirical formulas from Ref. [42] in Fig. 4. It is clear that the SST $k-\omega$ model can successfully reproduce the velocity and temperature profiles, while the realizable $k-\epsilon$ model has an overestimation problem. Hence, we conclude that the SST $k-\omega$ model is sufficiently accurate for mean-flow and temperature computation.

In order to ensure the grid independence, we carried out another two simulations by refining the basic grid by a factor of 1.5 at each direction. For the grid independence study, we have used the SST $k-\omega$ model. The horizontal variations of the normalized mean vertical velocity and temperature at the vertical location $z = H$ of these three grids are presented in Fig. 5. It can be seen that the difference in the results obtained using refined and basic grid is insignificant. However, the differences between the basic grid and the coarse grid cannot be ignored. Hence, concerning both the computational efficiency and accuracy, the grid setups of the basic grid are applied to the urban building simulations.

3. Results and discussion

3.1. Airflow structures

As the geometry of the city is symmetrical, it is intuitive to test whether the dynamical and scalar fields are also symmetrical. This is demonstrated explicitly by plotting velocity and concentration profiles at several symmetrical lines of $x/W = 1.0, 27, -1.0$ and -27.0 , where the geometrical symmetry axis of the city is located at $x/W = 0$. As shown in Fig. 6, the wind velocity profiles and concentration profiles at

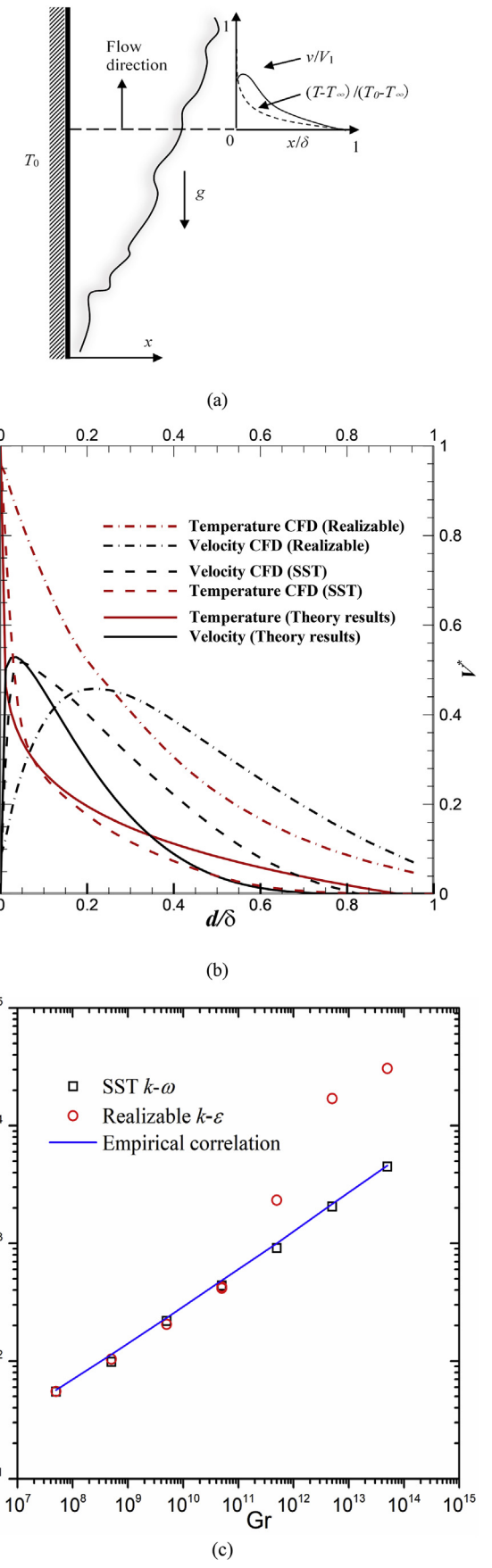


Fig. 4. Schematic of the physical configuration of the wall flow (a) and comparison between the results of empirical correlation and the present numerical simulation with the realizable $k-\epsilon$ model and SST $k-\omega$ model of the mean vertical velocity profiles (b) and surface Nusselt number (c).

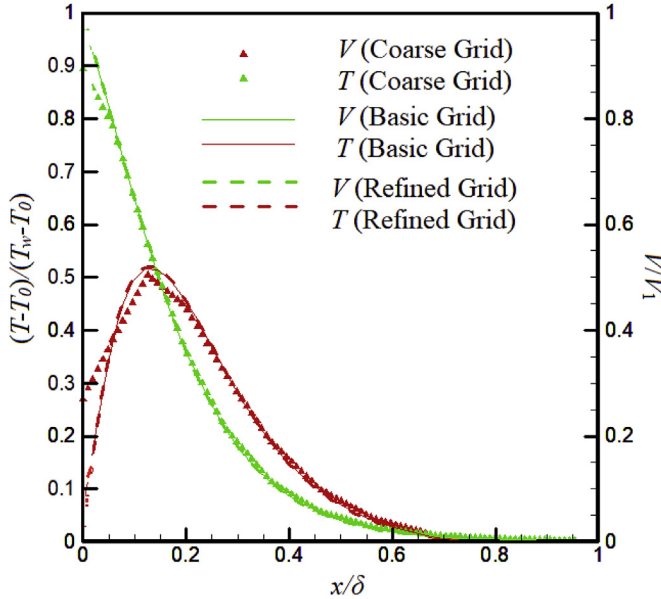
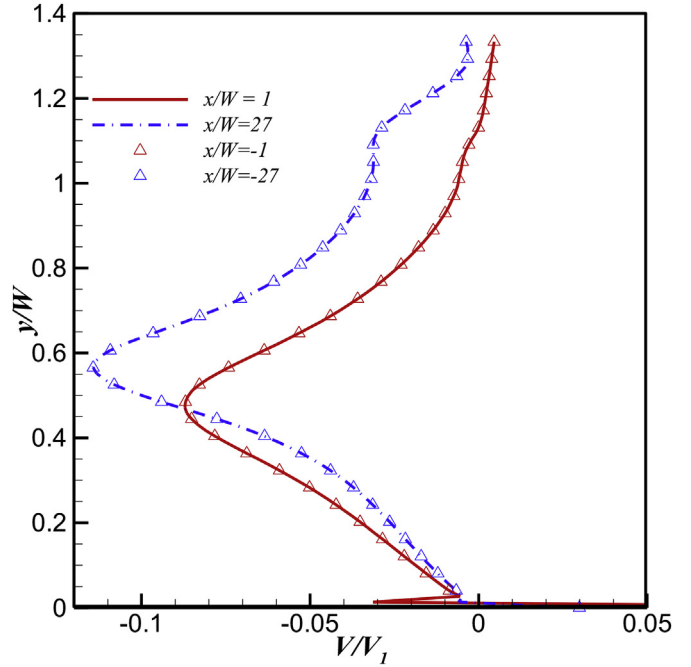


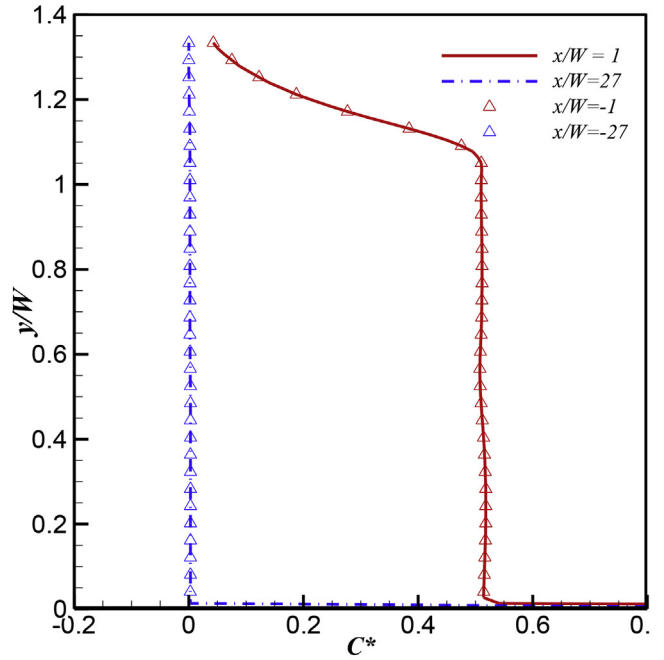
Fig. 5. Vertical velocity profiles along the line of ($z = H$, $x = 0$) for different grid distributions.

symmetrical positions are identical. Therefore, only half of buildings will be presented in the following parts. The horizontal and vertical directions are represented by the x and y coordinates respectively.

The airflow patterns inside the street canyon are firstly presented and discussed as they directly affect the pollutant dispersion processes. Fig. 7 shows the streamline fields when the temperature difference between building surfaces is 1 K. A horizontal convergence flow toward the urban center is observed above the canopy roof level. As a result, the flow field is similar to that at canyons, which is ventilated by combined dynamic and buoyancy force [44]. At mechanical induced canyon ventilation processes, the bulk of the above-roof flow does not penetrate in the canyon and a stable single vortex is established when the street is narrow, which is called the skimming flow (SF) pattern [21]. However, two counter-rotating vortices located diagonally in the street canyon are observed in uniform building height configurations. The ventilation mechanisms induced by the vertical wall flow are twofold: one ascent upwardly and merges with each other forming a horizontal convergence flow, while the other drives the vertically recirculating vortex within the street canyon. Lee and Park, (1994) [45] suggested that pollutant transport along streamlines was mainly due to advection by the mean wind, while pollutant transport across streamlines was mainly due to diffusion. Therefore, pollutants in outer streamlines can rapidly escape from the street canyon after being transported to the roof level, while pollutants near the vortex center require more time to escape from the street canyon. The upward motion near the upwind building is driven by buoyancy force, which reinforces the mechanical convergence flow at the canyon roof. On the contrary, the upward motion near the downwind buildings is of the opposite direction to the convergence flow, resulting with a secondary vortex near the downwind buildings. For the configurations with height variation, the flow structure inside the street canyon differs significantly from that within uniform configurations, which is also observed at previous wind driven scenarios [46]. When the building height variation is small, two vortices are generated at top of the short buildings. With the increase of the height variation, these two vortices merged with each other, forming a large vortex that extends from one tall building to the other. At the same time, a single vortex instead of two co-rotating is observed inside the street canyon. This is because the aspect ratio of the canyons with height variation is actually smaller than that with uniform height.



(a)



(b)

Fig. 6. Vertical profiles at two couples of symmetrical vertical lines (the symmetry axis is located at $x/W = 0$) for (a) normalized vertical velocity and (b) normalized pollutant concentration.

For configurations with the *protuberant* skyline, the overall urban morphology has a significantly effect on the local ventilation. Specifically, for canyons at urban center, the in-canyon vortex is stretch upwardly by the convergence flow. This may have a positive effect on diluting the pollutants at the urban center. For configurations with the *concave* skyline, the effect of overall urban morphology on the local canyon flow is insignificant. The convergence flow separates the in-

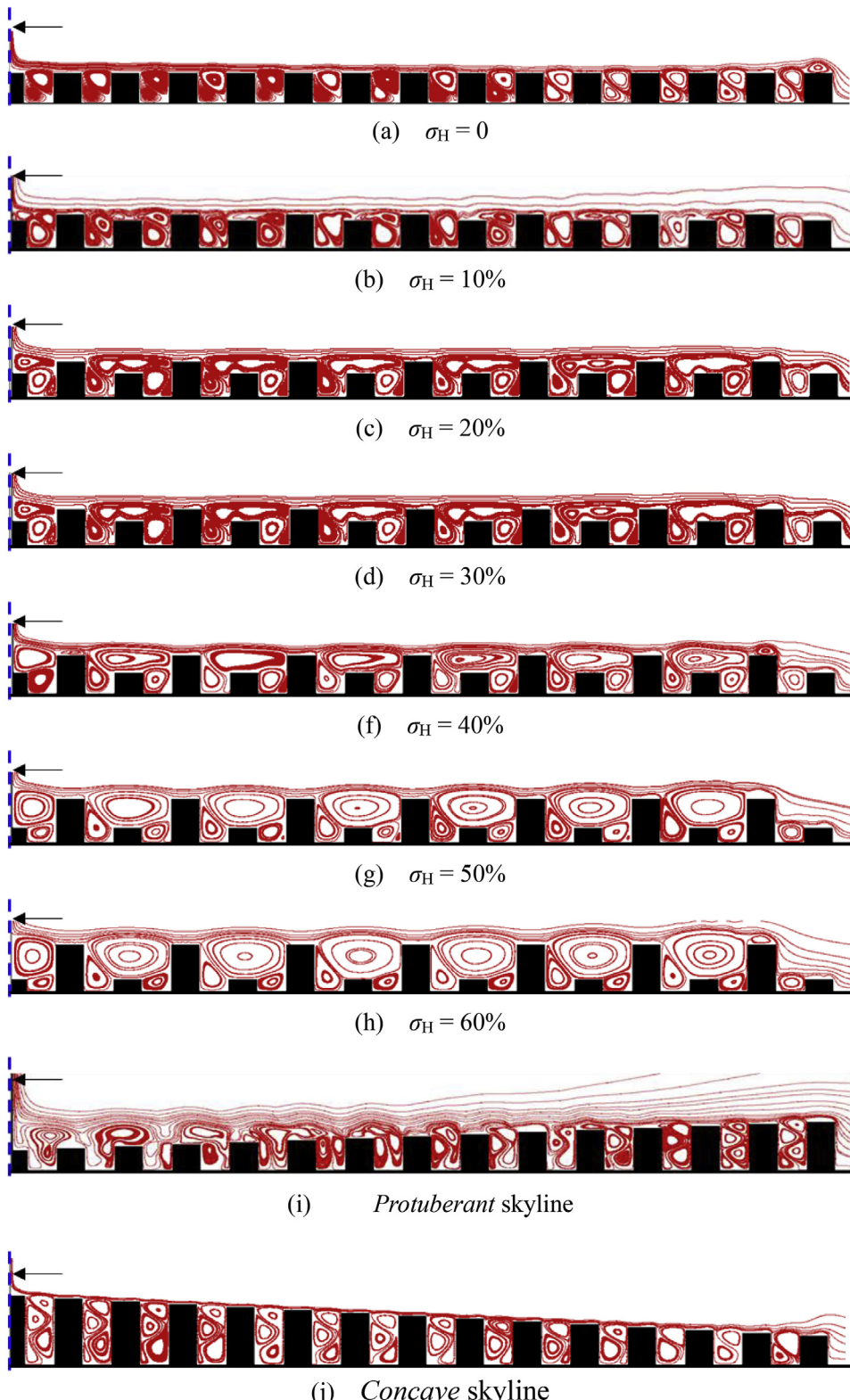


Fig. 7. Streamline field at different configurations with the buildings' surfaces heated to 1 K. Only half of the canyons are presented. The center lines are located at the left end of the figures, marked as blue dash lines. (For interpretation of the references to colour in this figure legend, the reader is referred to the Web version of this article.)

canyon space from the spaces above it. Multiple-vortices structure is formed below the canyon roof. The number of vortices inside the canyons ranges from two to four, which depend on the local aspect ratio.

3.2. Vertical flow fields

As the canyon ventilation is mainly induced by thermal buoyancy force, which is initially of vertical direction, the characteristics of the highly disturbed flow within and above the street canyon could be

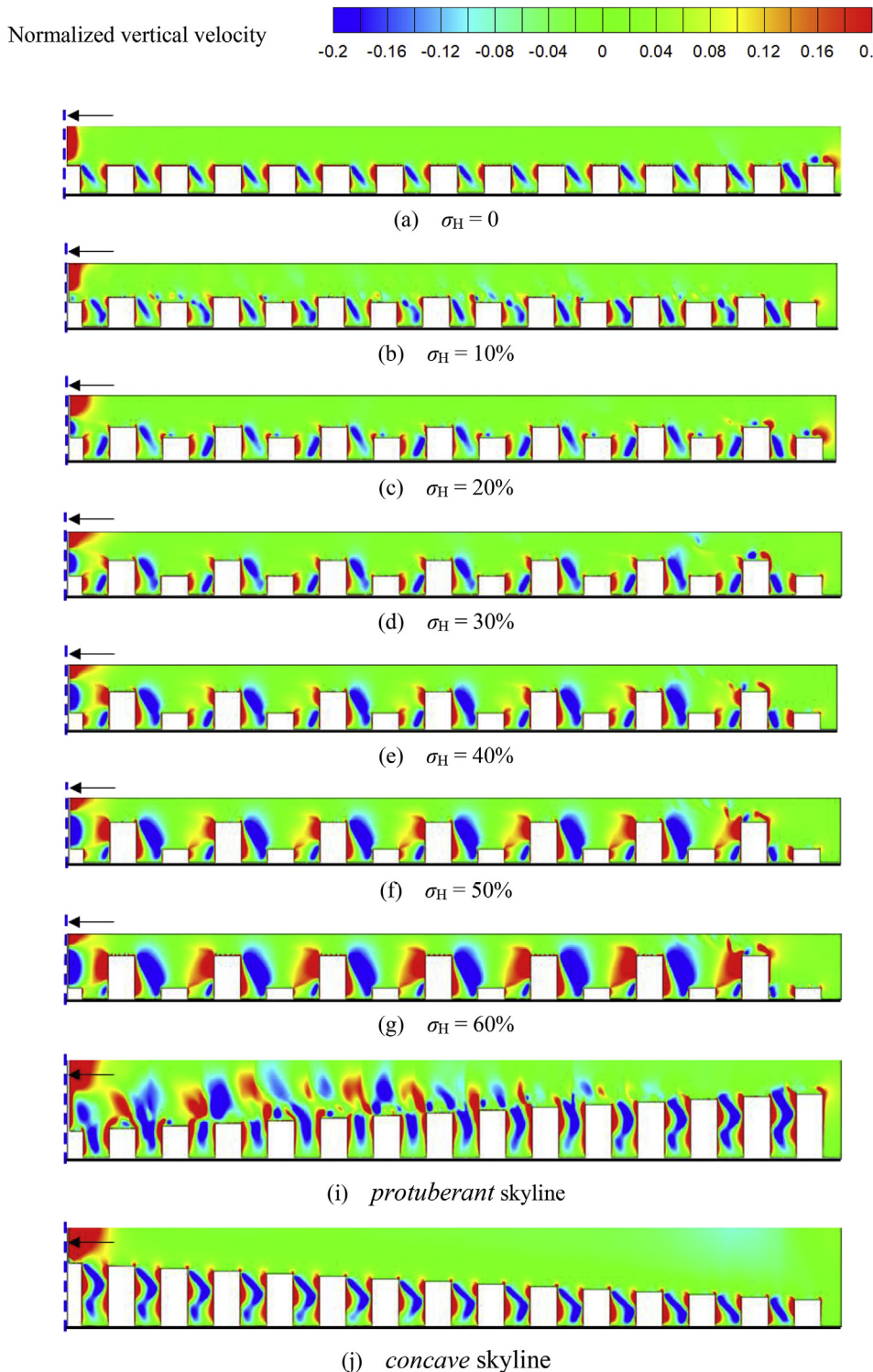


Fig. 8. Normalized vertical velocity field at different configurations with the buildings' surfaces heated to 1 K.

analyzed by using the contours of the mean vertical velocity, shown in Fig. 8. The mean vertical velocity is normalized by $V^* = V/V_{\max}$, where V^* and V is the normalized and original vertical velocity respectively. As is evident in Fig. 8, there are three distinct flow zones inside the street canyon: two upward movement zones (shown as red) formed in the immediate adjacency of the downwind and upwind surfaces and a downward movement zone (shown as blue) located between two upward zones. The downward movement hampers the development of the upward motion near the upwind surfaces, which disappears below the

roof level. As a result, polluted air could not be induced into the canyon volume at that position. For urban configurations with uniform building height, both the upward and downward motion are confined within a very narrow zone, where the $|V^*| > 0.2$. The rest space is calm with weak vertical movement. For urban configurations with building height variation, both the upward and downward motion zones are expanded significantly. For configurations with protuberant skyline, the upward motion zone at the urban center is significantly enlarged by the large scale motion. However, for configurations with concave skyline, the

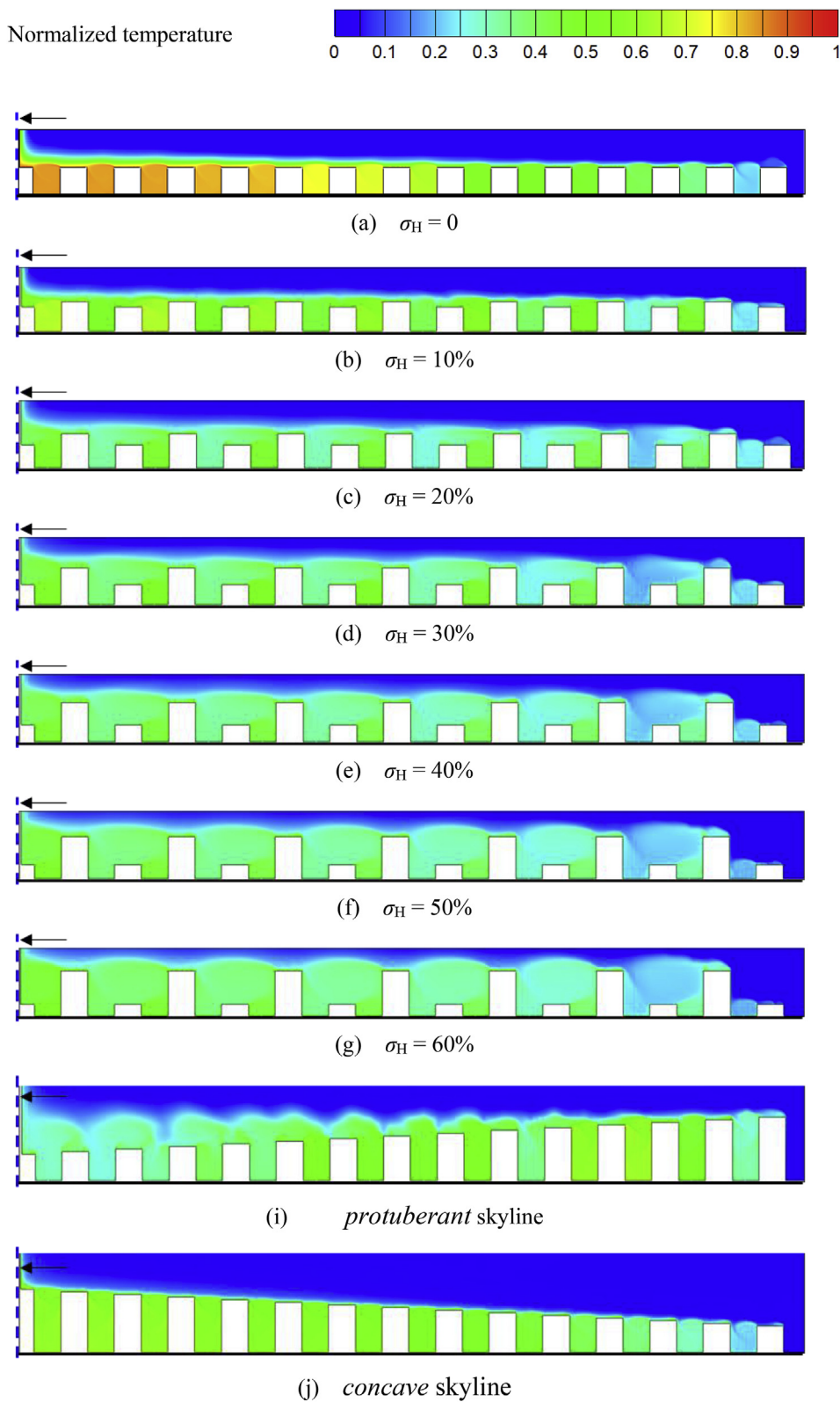


Fig. 9. Normalized temperature field at different configurations with the buildings' surfaces heated to 1 K.

upward and downward motion zones are confined within a very narrow zone at all canyons, which could have a negative effect on the removal of pollutants emitted near the ground.

3.3. Temperature fields

The distribution of the normalized mean air temperature is plotted in Fig. 9, which is calculated by $T^* = (T_s - T_a)/(T_s - T_a)$, where T_a is ambient air temperature and T_s the surface temperature of buildings. The plots show that the air temperature inside the canyon is heated to

achieve high temperature, which is approximately about $0.3\Delta T$. This temperature elevation is confined below the roof level. For the configuration with uniform building height ($\sigma_h = 0$), shown in Fig. 9(a), the air temperature in the urban center is much higher than that in the urban edge area. This could be caused by two potential mechanisms: (i) convergence flow at the roof level brings warm air from the urban edge area into the urban center area and (ii) convergence flow decays from urban edge area into the urban center area, resulting in a weak roof-level air exchange at urban center area. All of these will produce robust urban heat island intensity in the urban center. However, for the configurations with height variation, the air temperature in the urban center is much lower compared to that with a uniform building height. Hang et al. (2012) [16] suggested that height variation significantly enhanced air exchange at canopy ventilated by isothermal turbulent flows by enhancing the vertical mean flows. As shown in Fig. 7, the small counter-rotating vortices are stretched and merged into a large vortex, which enhance the mass mixing within the street canyon. For configurations with protuberant skyline, the heat accumulation at the urban center is alleviated, where the original vortices are stretched upwardly, and results in an increase of heat transfer rate at that position. For the configurations with concave skyline, the heat accumulation at urban center is very similar to that with the uniform building height.

In order to quantitatively investigate the effect of height variation on the in-canyon air temperature, the normalized spatially averaged air temperature is plotted against the height variation σ_h at Fig. 10. The air temperature is averaged over the street canyon volume, which is the space between the ground and the canyon roof. For street canyons at the center of urban area (Canyon 14), the spatial average air temperature gradually decreases with height variation when σ_h is smaller than 0.2, reaches its minimum value and keeps constant with further increasing σ_h . For street canyons at the edge of urban area, the spatially averaged temperature is hardly influenced by the height variation.

3.4. Evaluation of air exchange rate at canyon roof

ACH represents the rate of (aged) air removal from a street canyon through the roof level [47]. The implementation of ACH in street canyon air quality was firstly introduced by Ref. [35] using LES data. Then, Li and Leung, (2005) [48] modified the original concept so that the ACH can be calculated by the RANS models by assuming isotropic

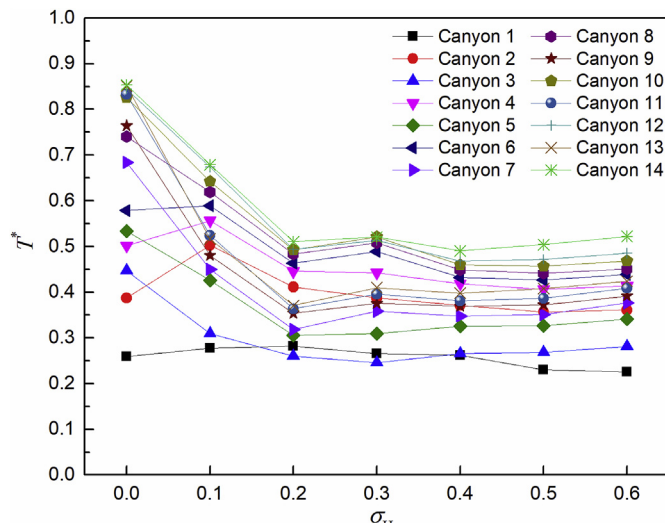


Fig. 10. Normalized canyon averaged temperature as a function of height variations. Canyon 1 is located at the rim of the urban and Canyon 14 is located at the urban center.

turbulence in their derivation. Recently, Cheng et al. (2008) [49] used the eddy-viscosity and -diffusivity models to derive the ACH , which is also applied in this study. The ACH can be divided into the mean component

$$\overline{ACH} = \int_{A_{roof}} |\bar{V}| dA \quad (15)$$

and the turbulent component

$$ACH' = \int_{A_{roof}} \frac{1}{2} \sqrt{\bar{V}' \bar{V}'} dA = \int_{A_{roof}} \sqrt{\left[\frac{k}{6} - \frac{1}{2} \nu_t \left(\frac{\partial \bar{V}}{\partial y} \right) \right]} dA \quad (16)$$

where V is the vertical velocity component and A_{roof} the roof area of the street canyon. The ACH has been replaced by normalized $ACH^* = ACH / U_{ref} A_{roof}$ as suggested, where $U_{ref} = V_1(\Delta T = 1 \text{ K}, H = 30 \text{ m})$.

In order to evaluate the correlation between the ACH to the temperature elevation at building surfaces and canyon position at the urban, a series of simulations with building surfaces heated to temperature ranging from 1 K to 20 K above the ambient air were conducted. The correlation between the ACH and the temperature elevation of the building surface is firstly evaluated mathematically by scale analysis. When the building geometry is unchanged, according to Eq. (15), the correlation between the wall flow rate Q and building surface temperature elevation is as follows:

$$Q \propto V_1 \propto Gr^{1/2} \propto (\Delta T)^{1/2} \quad (17)$$

To further evaluate the correlation between \overline{ACH} and wall flow rate Q , the \overline{ACH} is plotted against $(\Delta T)^{1/2}$ at Fig. 11(a), where Canyon 1 represents the first canyon located at the edge of urban area and Canyon 14 represents the canyon located at the center of urban area. A linear correlation between the \overline{ACH} and $(\Delta T)^{1/2}$ could be detected, indicating that the mean air exchange of the street canyon has a linear correlation with the wall flow rate Q . Besides, it could be observed that \overline{ACH}^* varies from canyon to canyon, and \overline{ACH} of canyons at the edge of urban area is higher than that at the center of urban area. This could be easily explained that the convergence flow is much stronger at the edge of urban area, and enhances the mean air exchange rate. Similarly, the normalized ACH^* is also plotted against the $(\Delta T)^{1/2}$ in Fig. 11(b). Also, linear correlation between ACH^* and $(\Delta T)^{1/2}$ could be found. In contrast to the \overline{ACH}^* , the difference between canyons no longer appears, indicating that the convergence flow has little effect on the turbulent flux at canyon roof. Based on these results, a semi-empirical correlation between ACH and temperature elevation is proposed here as

$$\begin{aligned} ACH &= \overline{ACH} + ACH' = aQ + bQ = c \times 0.146V_1\delta \\ &= c \times 0.146 \times 1.185 \frac{\nu}{H} (Gr)^{1/2} [1 + 0.494(\Pr)^{2/3}]^{-1/2} \end{aligned} \quad (18)$$

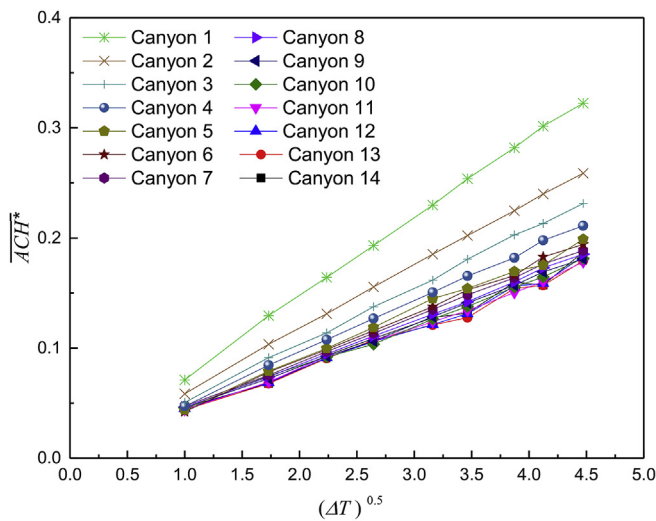
where the a , b and c are empirical parameters, and recommended as $a = 16.4$, $b = 11.5$ and $c = 27.9$ in this study. It should be noted that this correlation is based on configurations with uniform building height. The air exchange rate of street canyon at urban area with other skyline forms will be discussed in the following section.

3.5. Pollutant dilution within the street canyons

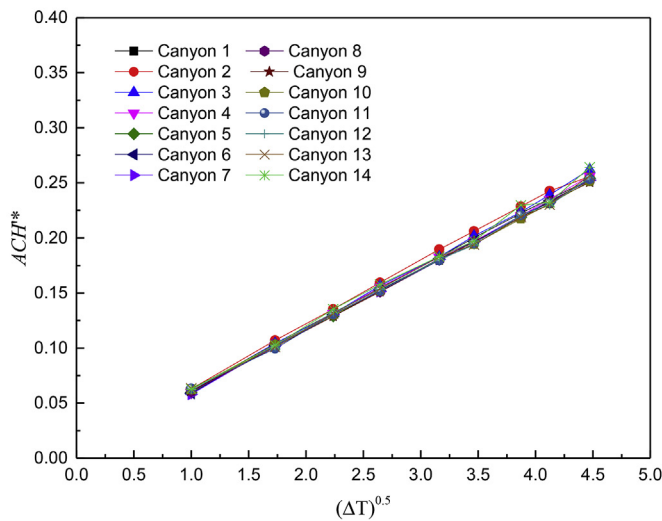
In this section, the dispersion characteristics of pollutants are investigated using the pollutant retention time proposed by Ref. [36], which is defined as the ratio of the total amount of pollutants remaining in the street canyon to the total amount of pollutants emitted. The pollutant retention time of the canyon is then defined as:

$$\tau_c^* = \frac{1}{Q_{emit}HW} \int_0^H \int_0^W C^* dA, \quad (19)$$

and the pollutant retention time at the pedestrian level ($z < H_p = 2 \text{ m}$) as is then defined as



(a) Air exchange rate due to mean flow



(b) Air exchange due to turbulent fluctuation

Fig. 11. Relationship between $(\Delta T)^{0.5}$ and the normalized air exchange rate \bar{ACH}^* (a) and ACH^* of the street canyon.

$$\tau_p^* = \frac{1}{Q_{\text{emit}} H_p W} \int_0^{H_p} \int_0^W C^* dA \quad (20)$$

It should be noted that the retention time is adopted as air-exchange estimation index, which should not be confused with the time of the pollutant parcel escape from the street canyons. In general, the concentration will depend on a number of processes. Nevertheless, this method could still provide some basic information about the near ground pollutant dilution processes.

For the wind driven urban ventilation, Mavroidis et al. (2012) [50] found a power law dependence of the pollutant residence time on the wind speed. Although they considered the residence time in the wake of an isolated cubic building, the airflow at present study within the street canyon is similar to that at the wake of cubes. Therefore, a similar correlation between pedestrian retention time and air exchange rate of street canyon is expected.

As $(\Delta T)^{1/2}$ has a linear relation with ACH , Fig. 12 shows variation of pollutant retention time of the street canyon τ_c with $(\Delta T)^{1/2}$ in semi-log plots. Although the retention time varies from canyon to canyon, the linear correlation between $\ln(\tau_c)$ and $(\Delta T)^{1/2}$ could be roughly established, except two canyons at the center of urban area where the oscillation occurs. Therefore, power low relation between τ_c and $(\Delta T)^{1/2}$

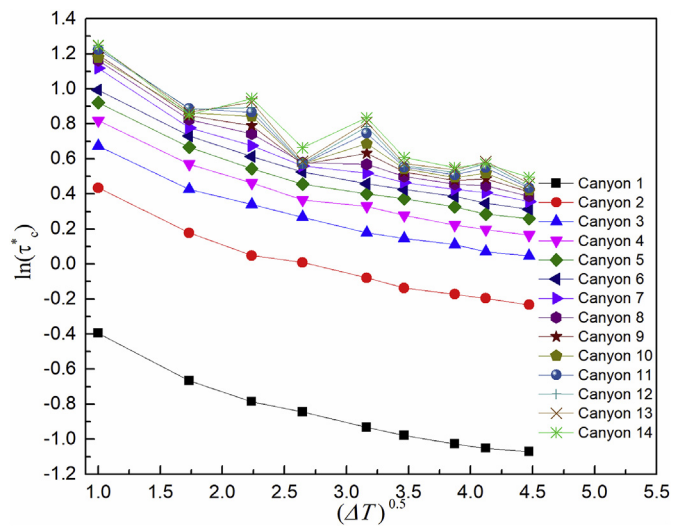


Fig. 12. Correlation between $(\Delta T)^{0.5}$ and the $\ln(\tau_c^*)$, where τ_c^* is the normalized canyon retention time.

derived by simple mathematical transformation, which is consistent with the previous findings [50]. The unperfected fitting is because that the horizontal convergence flow decays from urban edge to urban center. The difference between canyons in the retention time is so large that it is difficult to give an empirical correlation by simply give an empirical coefficient.

The distribution of non-dimensionalised mean concentration is plotted in Fig. 13. The computed concentrations were non-dimensionaized using the relation of $C^* = V_{\max} C / Q_{\text{emits}}$, where C is the concentration, V_{\max} is the maximum mean wind speed of the wall flow. The mean temperature and pollutant concentration distributions are exactly similar. Pollutants are accumulated into the urban center and this accumulation is alleviated by height variation.

The effect of height variation on the pollutant dispersion is then evaluated by the pedestrian retention time. Fig. 14 shows the variation of the pedestrian retention time with the height variation with for all the simulated cases with building surfaces heated to 1 K higher than ambient air. A strong dependence of the residence time on the canyon position is found. Canyons at the urban edge area experience a much lower pedestrian retention time compared to that at the center of urban area. Generally, height variation could reduce the pedestrian retention time, hence, improving the air quality. The pedestrian retention time at configurations with the *protuberant* skyline and the *concave* skyline is plotted at Fig. 15. For the configuration with *protuberant* skyline, the pedestrian retention time appears to present a maximum at the central axis and drops monotonously to the edge of urban area. The pollutant accumulation at urban area is serious. For the configuration with the *concave* skyline, the urban center experienced the lowest retention time as the in-canyon vortex is stretched upwardly. At the edge of urban area, due to strong convergence flow, the retention time is also at a low level. Due to the complexity of the vortex structure within the street canyon, the pedestrian level retention time shows a complicated variation trend. Specifically, the pedestrian retention time gradually increases with from the urban center to urban edge and attains a local maximum value, coincidentally at four canyons away from the urban center. This is then followed by a disrupt decrease and reaching a local maximum before increasing again until it reaches its maximum value and then eventually decreases again to the edge of urban area.

3.6. Limitations and suggestions for urban planners or designers

Obviously, many discrepancies still exist between the present idealized 2D street canyons and realistic 3D urban geometry in both air

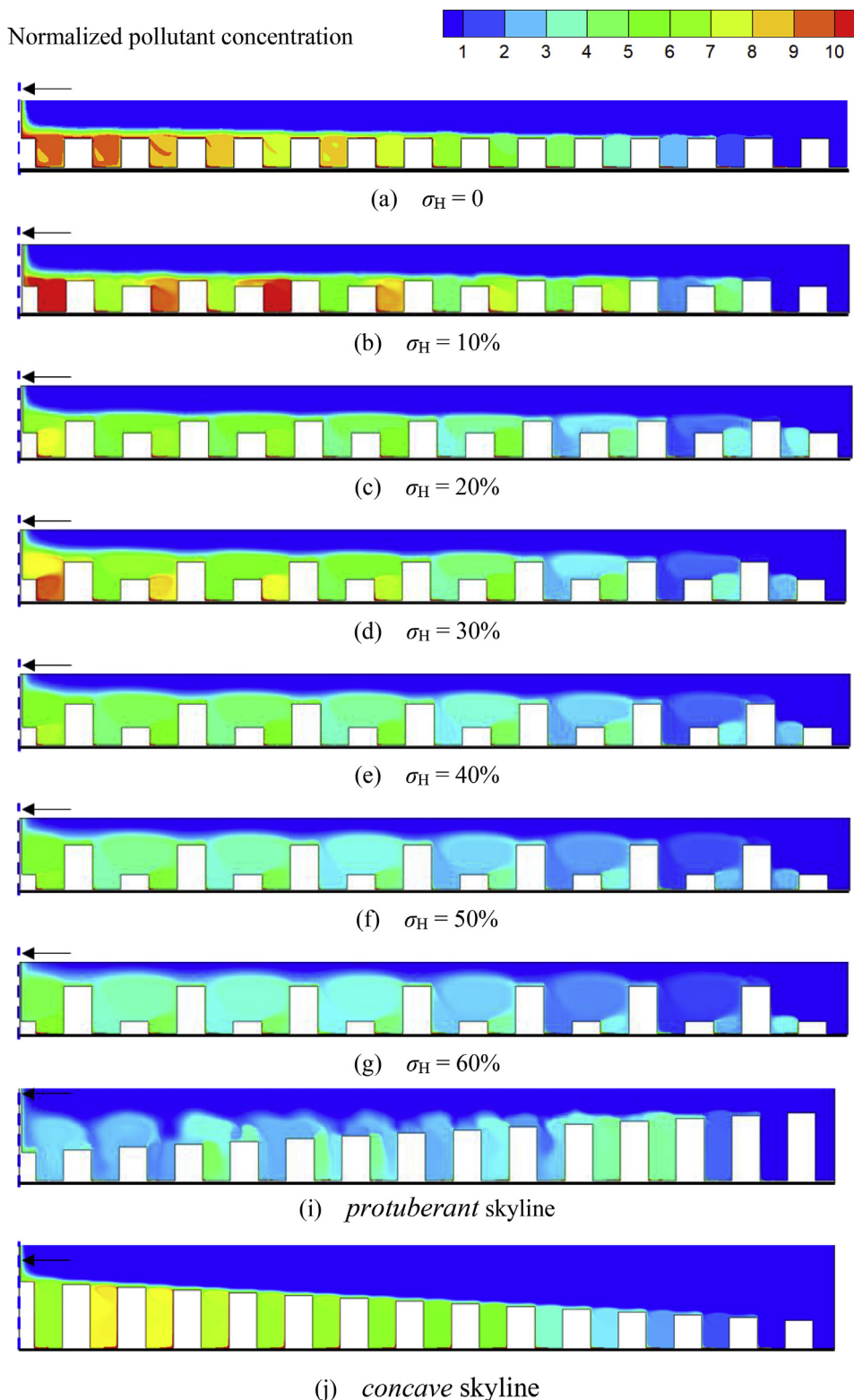


Fig. 13. Normalized pollutant concentration field at different configurations with the buildings' surfaces heated to 1 K.

temperature and wind flow. For example, channeling flow at streets with the same direction with the convergence flow may decrease the urban air temperature significantly. Clearly, further 3-D studies are still required before providing a practical framework for street design purpose. However, the present 2D simulation could still be valuable for urban plan and design as the main physical process of airflow, i.e., thermal plume merging, is included.

Based on the present study, the following suggestions are proposed for better urban air ventilation in a dense, hot-humid city:

- 1) Breezeways toward urban center should be provided in order to allow effective air movements toward the urban center to remove heat, gases and particulates and to improve the micro-climate of urban environment;

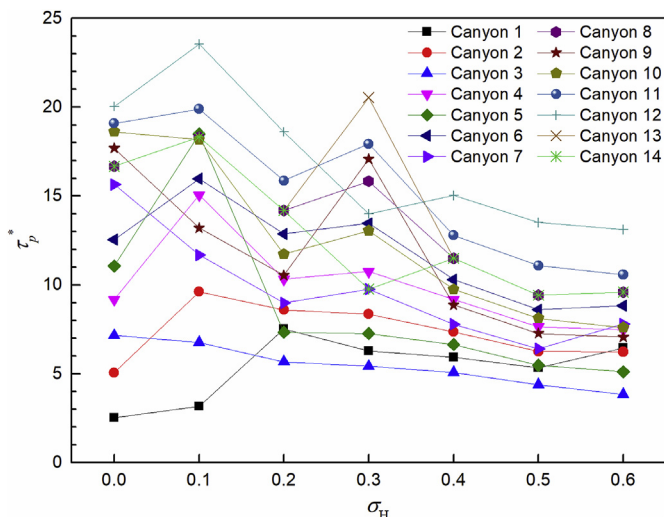


Fig. 14. Normalized pedestrian retention time as a function of height variations. Canyon 1 is located at the rim of the urban and Canyon 14 is located at the urban center.

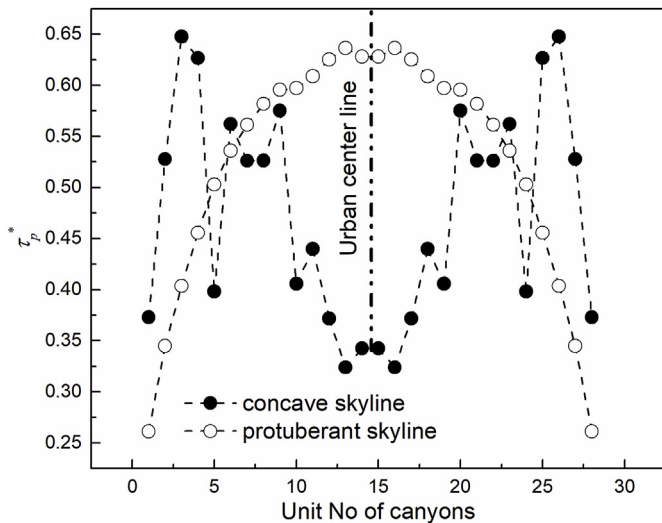


Fig. 15. Normalized pedestrian retention time at canyons of configurations with the “protuberant” skyline and the “concave” skyline.

- 2) Building height heterogeneity should be encouraged and uniform building height should be avoided;
- 3) If high-rise buildings must be built, it is better to build them at the urban fringe instead of urban geometrical center.

4. Conclusion

The air flow and pollutant dispersion within rows of street canyons ventilated by thermal buoyancy force resulting from the heated building surfaces are examined using the SST k- ω CFD model for different urban skyline configurations. Pollutants are emitted from the bottom of street canyons to mimic the traffic exhaust releasing. In addition to numerical investigations, theoretical modeling on the thermal boundary flow adjacent to a heated vertical wall is implemented.

Proposed theoretical solutions agree well with those discrete numerical ones. The air exchange rate (ACH) and pollutant retention time are applied to evaluate the canyon ventilation performance. To the best knowledge of authors, it is first time to present the theoretical evaluations on the air exchange rate at street canyon roof under the regime of pure buoyancy driven flows, exactly modeling such like haze weather

conditions. Theoretical correlations could provide a preliminary and general evaluation for the ventilation performance of street canyons under buoyancy driven wind flows.

Delicate numerical simulation results demonstrate that the air exchange rate due to mean flow is of linear relationship with the thermal boundary flow rate, although there exists little differences between canyons at different positions; whereas, air exchange rate due to turbulent fluctuation is also of linear relationship with thermal boundary flow rate, and particularly this relationship could be uniformly suitable for different canyons, i.e., it is independent of spatial arrangements.

A semi-empirical formula is proposed by the use of two constant empirical constants obtained from present simulation results, which could be used to estimate the ventilation performance of urban area at design stage. Additionally, an exponentially relationship between the pollutant retention time and thermal boundary flow rate is established. Whereas, straightforward relationship could not be established between the retention time and canyon locations due to the fact that the observed retention time differences between canyons at different position are much remarkable. The flow structure within the street canyon varies from canyon to canyon due to the interaction between local thermal driven flow and convergent flow induced by plume merging aloft the buildings.

The effect of urban skyline configurations on the residence time is also examined. Four categories of urban skylines were considered, including the uniform building height, staggered building height, protuberant and concave skyline. When the uniform building height slightly increases from 0.0 to 0.2, air exchange rate and pollutant retention time decay significantly; however, when the building height further increases, these two parameters are almost maintained unchangeable. For the protuberant skyline, high-rise buildings are locating at the urban city center. Wind flow and pollutant dispersion characteristics are very similar to those of uniform building height, except that the pollutant accumulation is exacerbated. For the concave skyline, the high-rise buildings are located at the urban edge area. The pollutant accumulation at urban center under this condition is alleviated as the in-canyon vortices are stretched upwardly tremendously.

Acknowledgements

This research was financially supported by the Natural Science Foundation of China (NSFC Grant No. 51778504, 51304233, 51208192), Fundamental Research Projects from Shenzhen Government (Grant No. JCY20160523160857948), and National Key Research and Development Program of the Ministry of Science and Technology of China (Grant No. 2018YFC0705201, Grant No. 2018YFB0904200).

Both Prof. Fu-Yun Zhao and Prof. Han-Qing Wang would also like to acknowledge the financial support from the Collaborative Innovation Center for Building Energy Conservation and Environment Control, Hunan Province.

References

- [1] H. Fernando, Fluid dynamics of urban atmospheres in complex terrain, *Annu. Rev. Fluid Mech.* 42 (2010) 365–389.
- [2] B.E. Boor, M.P. Spilak, J. Laverge, A. Novoselac, Y. Xu, Human exposure to indoor air pollutants in sleep microenvironments: a literature review, *Build. Environ.* 125 (2017) 528–555.
- [3] S.E. Belcher, Mixing and transport in urban areas, *Phil. Trans. Roy. Soc. Lond.: Math., Phys. Eng. Sci.* 363 (2005) 2947–2968.
- [4] R. Buccolieri, M. Sandberg, S. Di Sabatino, City breathability and its link to pollutant concentration distribution within urban-like geometries, *Atmos. Environ.* 44 (2010) 1894–1903.
- [5] R. Ramponi, B. Blocken, L.B. de Coo, W.D. Janssen, CFD simulation of outdoor ventilation of generic urban configurations with different urban densities and equal and unequal street widths, *Build. Environ.* 92 (2015) 152–166.
- [6] M.F. Yassin, Impact of height and shape of building roof on air quality in urban street canyons, *Atmos. Environ.* 45 (2011) 5220–5229.
- [7] S.J. Mei, C.W. Liu, D. Liu, F.Y. Zhao, H.Q. Wang, X.H. Li, Fluid mechanical

- dispersion of airborne pollutants inside urban street canyons subjecting to multi-component ventilation and unstable thermal stratifications, *Sci. Total Environ.* 565 (2016) 1102–1115.
- [8] J. Hang, Y. Li, Age of air and air exchange efficiency in high-rise urban areas and its link to pollutant dilution, *Atmos. Environ.* 45 (2011) 5572–5585.
- [9] J. Hang, Y. Li, R. Buccolieri, M. Sandberg, S. Di Sabatino, On the contribution of mean flow and turbulence to city breathability: the case of long streets with tall buildings, *Sci. Total Environ.* 416 (2012) 362–373.
- [10] J. Hang, Y. Li, M. Sandberg, R. Buccolieri, S. Di Sabatino, The influence of building height variability on pollutant dispersion and pedestrian ventilation in idealized high-rise urban areas, *Build. Environ.* 56 (2012) 346–360.
- [11] C. Tsang, K.C. Kwok, P.A. Hitchcock, Wind tunnel study of pedestrian level wind environment around tall buildings: effects of building dimensions, separation and podium, *Build. Environ.* 49 (2012) 167–181.
- [12] J. Hang, M. Sandberg, Y. Li, L. Claesson, Pollutant dispersion in idealized city models with different urban morphologies, *Atmos. Environ.* 43 (2009) 6011–6025.
- [13] R. Britter, S. Hanna, Flow and dispersion in urban areas, *Annu. Rev. Fluid Mech.* 35 (2003) 469–496.
- [14] J.J. Kim, J.J. Baik, A numerical study of the effects of ambient wind direction on flow and dispersion in urban street canyons using the RNG k-e turbulence model, *Atmos. Environ.* 38 (2004) 3039–3048.
- [15] S. Di Sabatino, R. Buccolieri, B. Pulvirenti, R. Britter, Simulations of pollutant dispersion within idealised urban-type geometries with CFD and integral models, *Atmos. Environ.* 41 (2007) 8316–8329.
- [16] J. Hang, M. Sandberg, Y. Li, Age of air and air exchange efficiency in idealized city models, *Build. Environ.* 44 (2009) 1714–1723.
- [17] S. Branford, O. Coceal, T. Thomas, S. Belcher, Dispersion of a point-source release of a passive scalar through an urban-like array for different wind directions, *Bound.-Layer Meteorol.* 139 (2011) 367–394.
- [18] O. Coceal, E.V. Goulart, S. Branford, T. Glyn Thomas, S.E. Belcher, Flow structure and near-field dispersion in arrays of building-like obstacles, *J. Wind Eng. Ind. Aerod.* 125 (2014) 52–68.
- [19] J.J. Kim, J.J. Baik, Urban street-canyon flows with bottom heating, *Atmos. Environ.* 35 (2001) 3395–3404.
- [20] Y. Nakamura, T.R. Oke, Wind, temperature and stability conditions in an east-west oriented urban canyon, *Atmos. Environ.* 22 (1988) 2691–2700.
- [21] J.F. Sini, S. Anquetin, P.G. Mestayer, Pollutant dispersion and thermal effects in urban street canyons, *Atmos. Environ.* 30 (1996) 2659–2677.
- [22] A. Kovar-Panskus, L. Moulinneuf, E. Savory, A. Abdelqari, J.F. Sini, J.M. Rosant, A. Robins, N. Toy, A wind tunnel investigation of the influence of solar-induced wall-heating on the flow regime within a simulated urban street canyon, *Water Air Soil Pollut. Focus* 2 (2002) 555–571.
- [23] X. Xie, C.H. Liu, D.Y. Leung, Characteristics of air exchange in a street canyon with ground heating, *Atmos. Environ.* 40 (2006) 6396–6409.
- [24] S. Magnusson, A. Dallman, D. Entekhabi, R. Britter, H.J.S. Fernando, L. Norford, On thermally forced flows in urban street canyons, *Environ. Fluid Mech.* 14 (2014) 1427–1441.
- [25] A.B. Barlag, W. Kuttler, The significance of country breezes for urban planning, *Energy Build.* 15 (1991) 291–297.
- [26] C. Georgakis, M. Santamouris, Experimental investigation of air flow and temperature distribution in deep urban canyons for natural ventilation purposes, *Energy Build.* 38 (2006) 367–376.
- [27] H.J. Fernando, D. Zajic, S. Di Sabatino, R. Dimitrova, B. Hedquist, A. Dallman, Flow, turbulence, and pollutant dispersion in urban atmospheres, *Phys. Fluids* 22 (5) (2010) 051301.
- [28] W. Cheng, C.H. Liu, D.Y. Leung, On the correlation of air and pollutant exchange for street canyons in combined wind-buoyancy-driven flow, *Atmos. Environ.* 43 (2009) 3682–3690.
- [29] Y. Fan, Y. Li, J. Hang, K. Wang, X. Yang, Natural convection flows along a 16-storey high-rise building, *Build. Environ.* 107 (2016) 215–225.
- [30] S. Yin, Y. Li, M. Sandberg, K. Lam, The effect of building spacing on near-field temporal evolution of triple building plumes, *Build. Environ.* 122 (2017) 35–49.
- [31] W. Wang, E. Ng, Air ventilation assessment under unstable atmospheric stratification - a comparative study for Hong Kong, *Build. Environ.* 130 (2018) 1–13.
- [32] S.H. Yim, J.C.H. Fung, A.K.H. Lau, S.C. Kot, Air ventilation impacts of the “wall effect” resulting from the alignment of high-rise buildings, *Atmos. Environ.* 43 (2009) 4982–4994.
- [33] C. Guney, S.A. Girkinkaya, G. Cagdas, S. Yavuz, Tailoring a geomodel for analyzing an urban skyline, *Lands. Urban Plann.* 105 (2012) 160–173.
- [34] B. Addepalli, E.R. Pardyjak, Investigation of the flow structure in step-up street canyons - mean flow and turbulence statistics, *Bound.-Layer Meteorol.* 148 (1) (2013) 133–155.
- [35] C.H. Liu, D.Y.C. Leung, M.C. Barth, On the prediction of air and pollutant exchange rates in street canyons of different aspect ratios using large-eddy simulation, *Atmos. Environ.* 39 (2005) 1567–1574.
- [36] R. Kumar, A. Dewan, URANS computations with buoyancy corrected turbulence models for turbulent thermal plume, *Int. J. Heat Mass Tran.* 72 (2014) 680–689.
- [37] M.Z.I. Bangalee, J.J. Miao, S.Y. Lin, Computational techniques and a numerical study of a buoyancy-driven ventilation system, *Int. J. Heat Mass Tran.* 65 (5) (2013) 572–583.
- [38] F.R. Menter, Two-equation eddy-viscosity turbulence models for engineering applications, *AIAA J.* 32 (1994) 1598–1605.
- [39] D. Jiang, W. Jiang, H. Liu, J. Sun, Systematic influence of different building spacing, height and layout on mean wind and turbulent characteristics within and over urban building arrays, *Wind Struct.* 11 (2008) 275–290.
- [40] J. Baker, H.L. Walker, X. Cai, A study of the dispersion and transport of reactive pollutants in and above street canyons—a large eddy simulation, *Atmos. Environ.* 38 (2004) 6883–6892.
- [41] C.S. Pant, A. Bhattacharya, A viscous sponge layer formulation for robust large eddy simulation of thermal plumes, *Comput. Fluids* 134 (2016) 177–189.
- [42] E. Eckert, T.W. Jackson, Analysis of Turbulent Free-convection Boundary Layer on Flat Plate, DTIC Document, 1950.
- [43] S.W. Churchill, H.H.S. Chu, Correlating equations for laminar and turbulent free convection from a vertical plate, *Int. J. Heat Mass Tran.* 18 (1975) 1323–1329.
- [44] X. Cai, Effects of differential wall heating in street canyons on dispersion and ventilation characteristics of a passive scalar, *Atmos. Environ.* 51 (2012) 268–277.
- [45] I. Lee, H. Park, Parameterization of the pollutant transport and dispersion in urban street canyons, *Atmos. Environ.* 28 (1994) 2343–2349.
- [46] B. Addepalli, E.R. Pardyjak, A study of flow fields in step-down street canyons, *Environ. Fluid Mech.* 15 (2) (2015) 439–481.
- [47] W.C. Cheng, C.H. Liu, D.Y.C. Leung, On the correlation of air and pollutant exchange for street canyons in combined wind-buoyancy-driven flow, *Atmos. Environ.* 43 (2009) 3682–3690.
- [48] X.X. Li, C.H. Liu, L.D.Y.C. Leung, Development of a k-e model for the determination of air exchange rates for street canyons, *Atmos. Environ.* 39 (2005) 7285–7296.
- [49] W.C. Cheng, C.H. Liu, D.Y.C. Leung, Computational formulation for the evaluation of street canyon ventilation and pollutant removal performance, *Atmos. Environ.* 42 (2008) 9041–9051.
- [50] I. Mavroidis, S. Andronopoulos, J.G. Bartzis, Computational simulation of the residence of air pollutants in the wake of a 3-dimensional cubical building. The effect of atmospheric stability, *Atmos. Environ.* 63 (2012) 189–202.